JOURNAL OF VIROLOGY, June 1990, p. 2768–2779
0022-538X/90/062768-12$02.00/0

Vol. 64, No. 6

Analysis of Experimental Mink Enteritis Virus Infection in Mink: In Situ Hybridization, Serology, and Histopathology

ÅSE UTTENTHAL,[1] STEEN LARSEN,[2] EBBA LUND,[1] MARSHALL E. BLOOM,[3] TORBEN STORGÅRD,[2] AND SOREN ALEXANDERSEN[2]*

Department of Veterinary Virology and Immunology[1] and Department of Veterinary Pathology,[2] Royal Veterinary and Agricultural University, 13 Bülowsvej, DK-1870 Frederiksberg C, Denmark, and Laboratory of Persistent Viral Diseases, Rocky Mountain Laboratories, National Institute of Allergy and Infectious Diseases, Hamilton, Montana 59840[3]

Received 21 December 1989/Accepted 21 February 1990

Strand-specific hybridization probes were used in in situ hybridization studies to localize cells containing mink enteritis virus (MEV) virion DNA or MEV replicative-form DNA and mRNA. Following the experimental MEV infection of 3-month-old unvaccinated mink, a significant increase in serum antibodies to MEV was detected at postinfection day (PID) 6, 2 days after the onset of fecal shedding of virus. Prior to the appearance of virus in feces, viral DNA could be detected in the mesenteric lymph node and intestine. The largest percentage of cells positive for virion DNA was 10% and was detected in the intestine on PID 6. However, replication of the virus apparently peaked at PID 4. The number of MEV replicative-form DNA and mRNA molecules was found to be approximately 250,000 copies per infected lymph node cell or crypt epithelial cell. The localization, levels, and time course of viral replication have important implications for the pathogenesis of MEV-induced disease. The data presented on MEV are correlated with earlier results on the other mink parvovirus, Aleutian mink disease parvovirus, and a possible explanation for the remarkable differences in pathogenesis of disease caused by these two parvoviruses is discussed.

Mink enteritis virus (MEV) is an autonomous parvovirus (14) causing an acute disease in mink. The disease was initially reported from Canada (33), where it caused a mortality of up to 80% of infected mink kits. The experimental infection causes a rapid and transient fecal shedding of virus (25, 32, 36) and an increase in specific serum antibodies shortly afterwards (36). Pathological changes in mink with either naturally occurring (16, 33) or experimental MEV infection (15, 25, 30) consist of lesions in the intestinal tract, spleen, and mesenteric lymph node. The degenerative phase is characterized by destruction of the crypts and villi, hyperemia, edema, and cell infiltration in lamina propria, and occasionally balloon cells or viral inclusions are formed. Spleen and lymph nodes are swollen and hyperemic, with degeneration of lymphatic cells. The distribution of virus in mink with MEV infection has not been investigated before, but the viral distribution during experimental infection of dogs with the closely related canine parvovirus (CPV) (18) has been investigated by using isolation in cell culture and subsequent immunofluorescence (19) or quantitation by hemagglutination (12). Direct immunofluorescence on cryostat sections of intestine has been employed (17) to determine the localization of the viral antigen. A plaque titration assay has been used to investigate the amount of infectious virus in intestine and lymph node tissues from mink experimentally infected with MEV 5 days prior to sampling (25).

We recently described a novel strategy involving strand-specific in situ hybridization to define target cells for viral replication by identifying cells containing specific nucleic acid intermediates of viral replication (4–6). The purpose of the study reported here was to study the tissue distribution of these viral nucleic acids, i.e., single-stranded virion DNA, double-stranded replicative forms (RFs) of DNA, and virus-encoded mRNA, and correlate these findings with the clinical, serological, and histopathological findings during an experimental MEV infection in mink.

* Corresponding author.

MATERIALS AND METHODS

Animals. A total of 11 15-week-old mink kits not carrying the Aleutian gene were used in the experiment. At this age, kits are still susceptible to experimental infection, while the majority of Danish mink are protected by vaccination programs. The mink were found free of circulating antibodies to Aleutian disease virus and MEV when tested by countercurrent electrophoresis (1, 13) and hemagglutination inhibition (HI) (36), respectively. The animals were housed separately in standard cages.

Viruses. The MEV inoculum was a generous gift from H. Kammer, United Animal Division, Madison, Wis. It was a 10% homogenate of spleen and intestine from MEV-infected mink and was identical to the inoculum used in a vaccination-challenge experiment reported earlier (36). The virus used in the laboratory test was the MEV-2 Ithaca strain (24) grown in Norden Laboratory feline kidney cells or in Crandell feline kidney (CRFK) cells, as described earlier (5, 36).

Experimental plan. Two randomly picked animals were killed before infection, and material from these animals was collected as control specimens. These mink are referred to as mink 0A and 0B. The remaining animals were given 1 ml of the virus inoculum by the oronasal route, and two animals were randomly picked and killed on postinfection days (PIDs) 2, 4, 6, and 8. The animals were labeled by the day they were killed followed by a letter, i.e., 2A and 2B, etc. One animal died on PID 6 and is referred to as 6C. The animals were examined clinically every second day.

Blood samples were collected from the cephalic vein 4 days before virus exposure, as described previously (8), and at necropsy.

Stool samples were collected before exposure and every

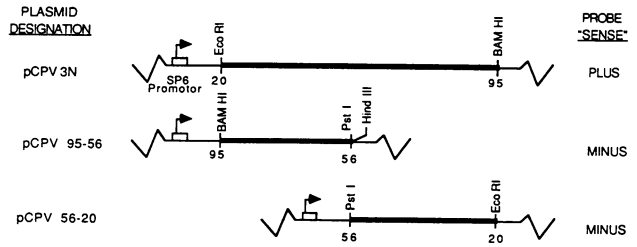

FIG. 1. Summary of the single-stranded RNA hybridization probes. A 20- to 95-m.u. fragment of the CPV genome was cloned into the SP6-based transcription vectors pSP64 and pSP65, as described previously (11). The vector synthesizing the plus-sense transcript is designated pCPV3N, and the two subclones transcribing the minus-sense transcripts are designated pCPV95-56 (spans 95 to 56 m.u.) and pCPV56-20 (spans 56 to 20 m.u.). Purified plasmid DNAs were linearized downstream of the viral sequences at the *Bam*HI, *Hin*dIII, and *Eco*RI sites and used as templates in in vitro SP6 transcription reactions (5, 11). The locations of the SP6 promoter and the restriction enzyme sites used in the cloning and probe preparation procedures are indicated.

second day after exposure. Both stool and serum samples were frozen and kept at −20°C until assayed.

The animals were killed by exsanguination under pentobarbital anesthesia. Pieces of heart, lung, liver, spleen, kidney, mesenteric lymph node, and defined areas of duodenum, jejunum, and ileum were immediately fixed in freshly prepared ice-cold periodate-lysine-paraformaldehyde-glutaraldehyde (PLPG) solution as previously described (4, 5). Serology only was performed on the animal found dead on PID 6, because fresh material was required for hybridizations. Fixed tissues were embedded in paraffin, and sections were made for in situ hybridizations and histological examination as described previously (4, 5). The blood samples were taken in plain tubes to prepare sera. Bile was collected from the gallbladders of killed animals.

Hybridization probes. All enzymes, isotopes, vectors, and other chemicals were from sources previously enumerated (3–6, 11).

Single-stranded sense-specific RNA hybridization probes were developed by subcloning a 20- to 95-map-unit (m.u.) fragment of the CPV genome (kindly provided by Colin Parrish, Cornell University, Ithaca, N.Y.) into a transcription vector based on bacteriophage SP6 (5, 11). CPV is more than 95% related to feline panleukopenia virus and to MEV at the DNA level (18, 22, 25, 29, 31, 34), and therefore a probe based on CPV DNA can be used for detection of CPV-, feline panleukopenia virus-, and MEV-encoded nucleic acids. The vector synthesizing a plus-sense transcript (pCPV3N) was obtained directly, as schematically represented in Fig. 1. However, in order to obtain a vector generating a minus-sense transcript, it was necessary to generate two subclones by cutting the 20- to 95-m.u. fragment at the *Pst*I site at m.u. 56 (22, 23) and clone the two pieces into the transcription vector (Fig. 1). Radiolabeled RNA transcripts from these two clones (pCPV95-56 and pCPV56-20) were mixed to obtain a representative minus-sense probe. For details on cloning procedures, see references 5 and 11.

Single-stranded RNA probes were transcribed in vitro under conditions previously detailed (5, 11). For filter blot hybridizations, the RNA was radiolabeled with [^{32}P]UTP; for in situ hybridization, the RNA was radiolabeled with [^{35}S]UTP as detailed previously (5, 11). The sizes of the transcripts were verified by the electrophoresis of a portion of the labeled RNAs in a formaldehyde-agarose gel, detection by autoradiography, and size estimation by comparison with included standards (5, 11).

Sense specificity of the probes. The sense specificity of the probes was tested by hybridization to replicate Southern blots of whole-cell DNA containing a known amount of MEV DNA or to Northern (RNA) blots of poly(A)-selected MEV mRNA isolated from MEV-infected CRFK cells, as described previously (3, 5, 11). The plus-sense probe reacted with both single-stranded virion DNA and double-stranded RFs of MEV DNA but did not react with MEV mRNA (data not shown). In contrast, the minus-sense probe reacted primarily with the RFs of DNA and also with MEV mRNA. These findings suggested that the minus-sense probe could be used preferentially to detect replication of the virus (presence of RFs of DNA and mRNA), while the plus-sense probe could be used preferentially to show the mere presence of virus (virion DNA). For a detailed discussion of strand-specific probes, the reader is referred to previous papers (3–6, 9, 11).

The data also showed that the CPV probe, as expected, cross-hybridized with excellent specificity and sensitivity to MEV sequences.

In situ hybridization techniques. The in situ hybridizations were performed exactly as described previously (4–6), except that the CPV probes were used. Quantitation of genome copy numbers was done as described previously (4–6).

Detection of viremia and virus in feces by hybridization. Serum samples (200 μl) diluted 1:1 in TNE (0.15 M NaCl, 0.01 M Tris [pH 7.4], 0.001 M EDTA) and fecal samples (1 ml of a 20% suspension) were supplied with 1 μg of sheared salmon sperm DNA as a carrier. DNA was then isolated by the sodium dodecyl sulfate-proteinase K digestion method described previously (10). The DNA was transferred to nylon membranes (Hybond-N; Amersham Corp., Arlington Heights, Ill.) by using standard Southern blot or slot blot techniques. Filters were hybridized with the ^{32}P-radiolabeled plus-sense CPV RNA probe as described previously (2–5, 10, 11). As an internal standard, 0.5 ng of purified MEV RF DNA was applied to the membranes.

Viral antigen determinations. The amount of viral antigen in stool and urine samples was tested by sandwich enzyme-linked immunosorbent assay (ELISA), as described previously (36). A known positive fecal sample was included as an internal standard. The ELISA values of the positive wells (wells with rabbit anti-MEV as the catching antibody) minus the negative wells (wells coated with nonimmune rabbit sera) were indexed according to the positive control. Samples containing more than 20% of the standard value were considered positive for MEV antigen.

Antibody titrations. Antibodies to MEV in serum and bile samples were tested by HI on African green monkey erythrocytes in barbital acetate-buffered saline (pH 6.2), as described previously (36).

RESULTS

Clinical signs and viral excretion. The animals remained healthy until PID 4, when five of seven mink (4B, 6A, 6B, 6C, and 8A) had diarrhea and stopped eating. Mink 6C was found dead on PID 6.

The virus antigen content was analyzed in stool samples from the number of animals still alive on the sampling day. This means that PID 0 represents samples from 11 animals, PID 2 represents 9 samples, PID 4 represents 7 samples, PID 6 is 5 samples, and PID 8 is based on 2 samples. Fecal

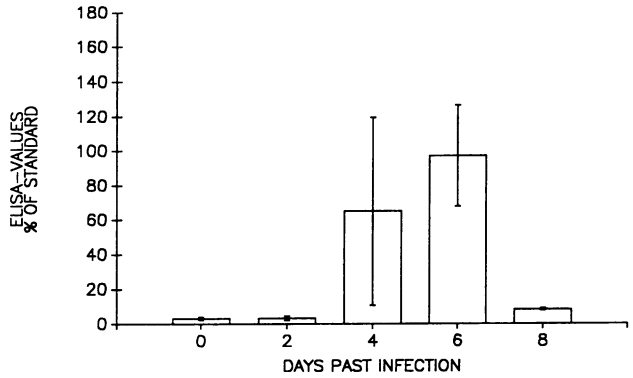

FIG. 2 Amount of viral antigen in stool samples measured by sandwich ELISA as described in Materials and Methods. The means and standard deviations for the days indicated are presented. The number of samples tested was as follows: PID 0, 11 samples; PID 2, 9 samples; PID 4, 7 samples; PID 6, 5 samples; and PID 8, 2 samples. All stool samples were indexed to an internal standard of 100%, and the means were calculated from these results.

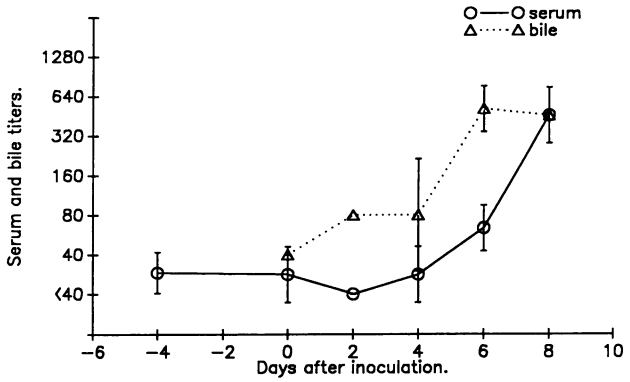

FIG. 3. Specific antibody titers in serum and bile measured by HI analysis of erythrocytes from the African green monkey. Blood samples were taken from all 11 animals 4 days prior to infection. After infection, two animals were killed every second day and serum and bile were obtained at necropsy. The results are presented as the mean value and standard deviation of the two samples.

samples were tested individually and compared with the internal standard, and the mean and standard deviations were calculated from the percentages in the individual samples. The results are shown in Fig. 2.

During the first 2 days following inoculation, none of the stool samples contained antigen in excess of background (i.e., >20%). At PID 4, the mean antigen content as a percentage of the standard was more than 60%, but the standard deviation was very large, indicating that some of the animals had more than 100%, and some had not yet started to excrete virus. All samples taken at PID 6 contained large amounts of antigen. On PID 8, the antigen content decreased and both samples were near the detection limit.

The DNA hybridization analysis of fecal samples revealed almost identical results. By DNA hybridization, four ELISA-negative samples showed a positive reaction. The results were concordant in 21 negative and 9 positive samples, giving an agreement of 88% in the 34 samples.

Antibody titrations. Four days prior to infection, serum samples were taken from all animals, and all samples were negative in HI tests (<40). The antibody content in serum remained below the detection limit until PID 6, when two of three animals had a slight elevation in antibody titer. On PID 8, both animals had an antibody titer of >320.

The antibody titer in bile was measured by the method mentioned above. This testing revealed some problems during the preabsorption of bile samples with monkey erythrocytes, because of the hemolytic effects of bile. During preabsorption, the erythrocytes were lysed, but the following HI test showed no inhibition in bile on PID 0. From PID 2, there was a significant increase in HI titers and the titer in bile increased at least as fast as it did in serum. The results of both serum and bile titrations are presented in Fig. 3.

Detection of viremia by hybridization. Viremia was detectable only in animals 2A, 4B, and 6C. The amount of MEV virion DNA in mink 6C was about 10 ng/ml of serum, or approximately 5 x 10^9 viral genomes per ml. The amount of viral DNA in serum samples from mink 2A and 4B was about 10-fold lower than the amount in the sample from mink 6C.

In situ hybridization analysis of infected cell cultures. In situ hybridization analysis was performed on control (uninfected) and MEV-infected CRFK cells by using the strand-specific probes. No grain count over background could be detected over uninfected cells or cells infected for 6 h by using either probe. At 10 h postinfection (p.i.), a few grains over background were found over cells and the number of grains per cell increased with time and reached maximum levels at 24 h p.i. At 48 h p.i., the number of grains per cell was still high, and in addition, a new population of cells containing fewer grains was found, indicating new cell-to-cell spreading of the virus infection. At 72 h p.i., up to 50% of the cells were positive for viral sequences.

By using the plus-sense probe, we found that the grains were located in the nuclei of infected cells in early infection but that later they became progressively located in the cytoplasm (Fig. 4). When cells were pretreated with RNase and hybridized to the minus-sense probe (shows RFs of DNA), grains were located in the nuclei at all time points, except for cells falling apart at late time points (Fig. 4). When cells were not pretreated with RNase, the minus-sense probe preferentially detects viral mRNA (4, 6) and the location of the grains at all times was mainly cytoplasmic (Fig. 4). The number of grains over cells infected for 24 h was counted, and the number of copies of viral nucleic acid sequences was estimated as described previously (4–6). On the basis of these estimations, infected cells contained approximately 50,000 to 100,000 copies of viral single-stranded DNA genomes and the same amount of double-stranded RFs of DNA and, in addition, 250,000 to 300,000 copies of viral mRNA.

In situ hybridization analysis of infected mink tissues. Sections from all mink killed during the experiments were hybridized in situ by using the strand-specific probes. Sections were not pretreated with RNase, and therefore grains over cells using the minus-sense probe represented viral RFs of DNA and viral mRNA suggestive of viral replication in the cell, while grains with the plus-sense probe in tissue areas negative with the minus-sense probe primarily represented the mere presence of virion DNA either previously produced in the cell or just being sequestered at the site.

Sections from control mink consistently gave low levels of grains diffusely distributed over the whole slide and established the background level (Fig. 5). Infected CRFK cells (24 h p.i.) with a known number of MEV genomes per positive cell were included in each hybridization and served as an internal standard by which copy numbers could be calculated (4–6).

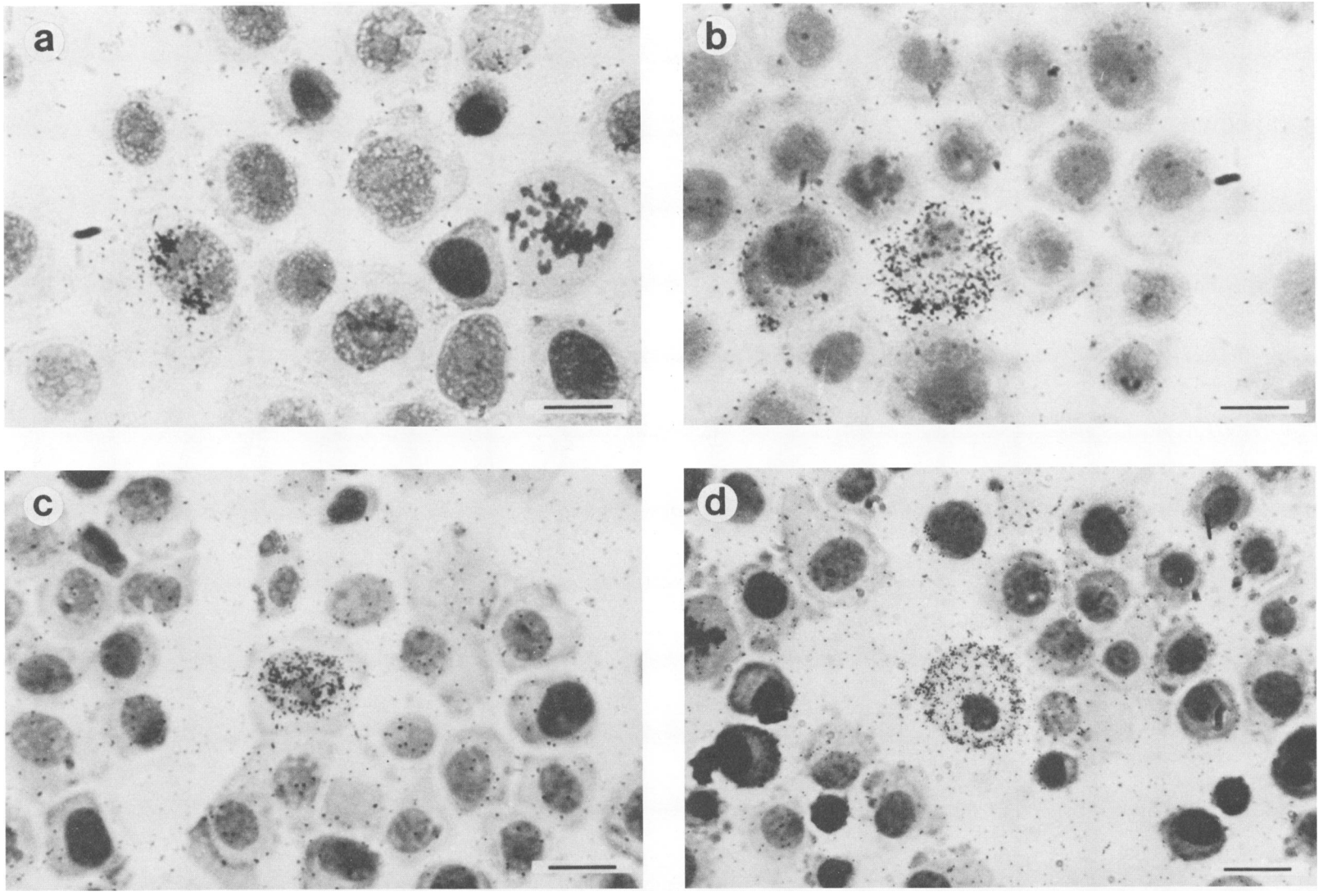

FIG. 4. In situ hybridization analysis of MEV-infected CRFK cells. (a) In situ hybridization analysis of PLPG-fixed CRFK cells infected with MEV for 10 h. The cells were pretreated with RNase and hybridized with the minus-sense probe. Grains can be observed in two discrete areas in the nucleus of an infected cell. (b) In situ hybridization analysis of cells infected for 14 h and not pretreated with RNase. The cells were hybridized with the minus-sense probe. Grains, representing hybridization to viral mRNA, can be observed in the cytoplasm of an infected cell. (c) In situ hybridization analysis of CRFK cells infected with MEV for 18 h and hybridized with the plus-sense probe. Grains are seen over the nucleus of an infected cell. (d) In situ hybridization analysis of cells infected with MEV for 24 h and hybridized with the plus-sense probe. Grains are seen over the cytoplasm of an infected cell. Bars, 13 μm.

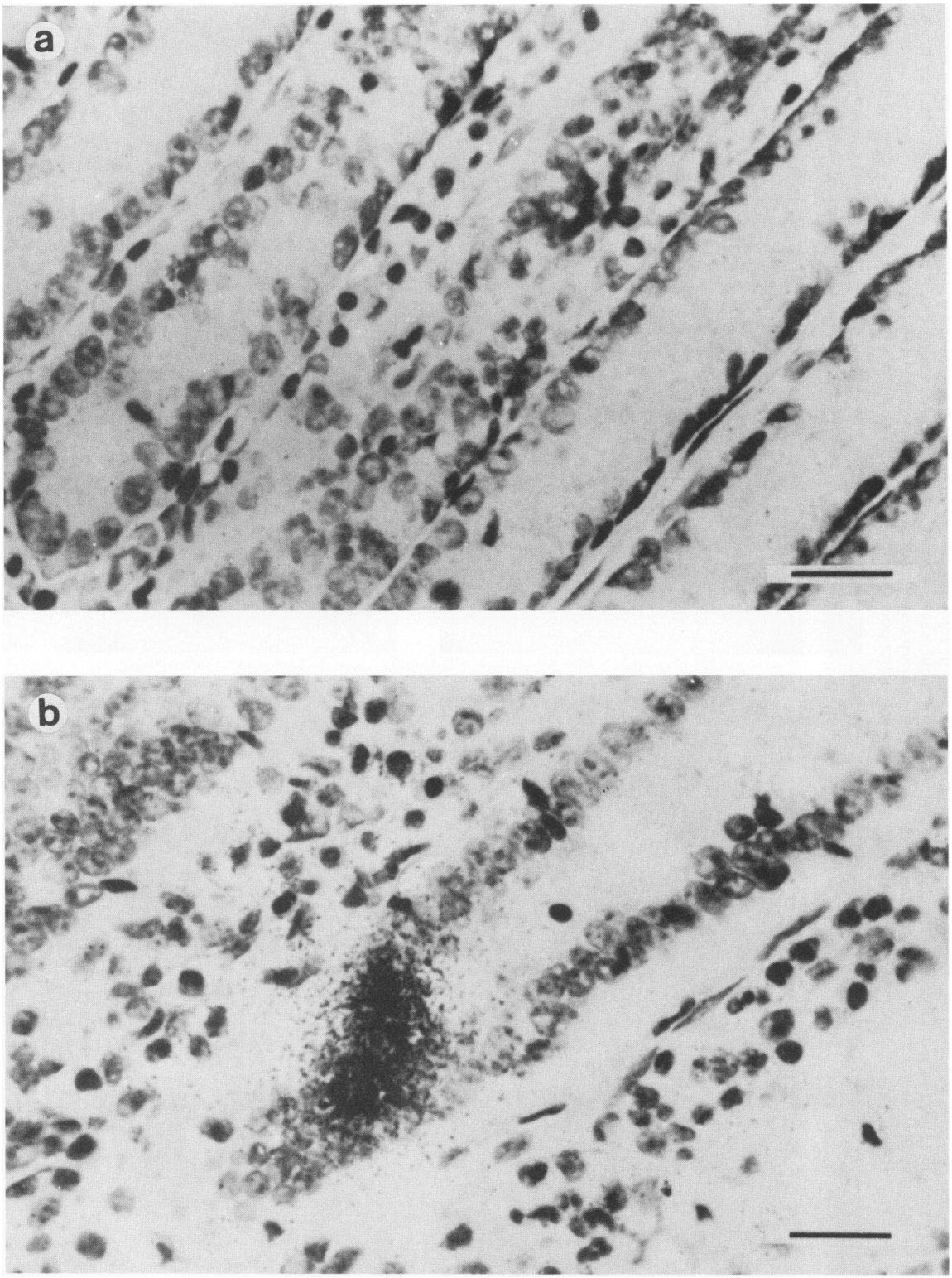

FIG. 5. In situ hybridization analysis of sections of ileum from noninfected (control) and MEV-infected mink. (a) In situ hybridization analysis of ileum section from a normal (control) mink using the plus-sense probe. Only background levels of grains can be detected. (b) In situ hybridization analysis of ileum section from a mink infected with MEV for 2 days. The section was hybridized with the plus-sense probe. Heavy grain formation can be observed over a few epithelial cells in the bottom of a crypt. Bars, 20 μm.

By using either of the probes, on PID 2 it was observed that grains in excess of background were formed over cells in the crypt area of the ileum (Fig. 5) and in the middle of germinal centers in the mesenteric lymph node. The other organs and the duodenum and jejunum sections of the intestine were negative for MEV sequences. At PID 4, maximum levels of viral replication (i.e., detection of viral RFs of DNA and mRNA) were detected in mesenteric lymph node cells (Fig. 6) and in crypt epithelial cells of the ileum (Fig. 7) where up to 2 to 5% of the total cell population was positive with the minus-sense probe. At this time, viral replication could also be detected in crypt cells of the duodenum and jejunum. However, fewer cells were affected in these areas of the intestine. The spleen contained a few positive cells scattered throughout the parenchyma. The positive cells of the mesenteric lymph node consisted of a few scattered single cells in the cortex region and a high concentration of positive cells in the periphery of the central zones of lymph node follicles. These cells could not be identified with certainty, but the location is characteristic of stimulated B lymphoblasts, although T cells, dendritic cells, and macrophages may also be found at these sites (28, 37, 38). The other organs were negative for viral replication at this time (PID 4). However, the plus-sense probe reacted with a small number of cells in the liver, indicating the mere presence of virus in this location. The positive cells had a morphology and localization resembling Kupffer cells. With this probe, areas around the germinal centers of the mesenteric lymph node and around the central arteries of the spleen were diffusely positive for sequestered viral DNA sequences. At PID 6, the level of viral replication was decreased but the level of viral single-stranded DNA had reached peak values (Fig. 7). At PID 8, viral replication decreased even further and only a few (approximately 0.1%) of the cells in the mesenteric lymph node and intestine were positive for active viral replication, although up to 2% of the cells still contained single-stranded viral genomes. At this time, most of the virus was located around germinal centers of the mesenteric lymph node, while very little of the virus was located in the lymph node sinuses. In the intestine, most of the virus was located in desquamated epithelial cells, in the intestinal lumen, or in the gut-associated lymphoid tissue of the ileum (Fig. 8).

The quantitative data of the experiments are summarized in Table 1 and in Fig. 9. Only the data for the ileum are shown; the kinetics of viral replication in the mesenteric lymph node were very similar, although fewer cells became infected.

Histopathology. No significant lesions were found in control (uninfected) mink or in mink killed on PID 2. On PID 4, a widespread, irregularly distributed loss of crypt epithelial cells and moderate-to-severe villous atrophy were conspicuous in the duodenum and ileum sections but less severe in the jejunum sections. Affected crypts were lined by variably attenuated epithelial cells, many of which contained intranuclear, eosinophilic, or amphophilic homogeneous or slightly granular accumulations compatible with viral inclusions. The crypt lumen contained desquamated cells, mucin, and a few—mainly eosinophilic—granulocytes. Lesions were also found in the mesenteric lymph node and to a lesser degree in the spleen. These lesions consisted of cellular necrosis with nuclear debris and an apparently intercellularly located eosinophilic, proteinaceous material in several germinal centers. Occasional cells in germinal centers or in the corona of surrounding lymphocytes in the mesenteric lymph node contained intranuclear accumulations compatible with viral inclusions. On PID 6, the lesions of the intestine consisted of patchily distributed loss of crypt epithelial cells, villous atrophy (Fig. 10), and accumulation of cellular debris in the crypt lumens as described for PID 4. In addition, occasional villi and crypts in the duodenum and ileum had epithelium with voluminous, finely vacuolated cytoplasm i.e., ballooning change. Several viral inclusions (Fig. 10) were observed in crypt epithelial cells of the ileum, and a few inclusions were observed in the jejunum. In the mesenteric lymph node, many hypocellular germinal centers had intercellular, eosinophilic, and proteinaceous accumulations. No viral inclusions were observed. At PID 8, lesions were most severe in the ileum where many irregularly distributed and often slightly dilated, atrophic crypts were lined by attenuated or ballooning epithelium. This ballooning change was also observed in villous epithelium covering atrophic villi. Occasional viral inclusions were observed in affected crypts. The lesions of the duodenum and especially the jejunum were less pronounced and consisted of scattered crypts with variable dilated lumen and attenuated epithelial lining and containing cellular debris and a few inflammatory cells. Viral inclusions were not observed. The lesions of the mesenteric lymph node were as described for PID 6. No significant lesions were found in any of the other organs examined.

DISCUSSION

In this study, the level and cellular localization of virus replication and sequestration during an experimental MEV infection of mink were examined by nucleic acid hybridization techniques. The data were correlated with the findings by using conventional serological and histopathological methods to get a detailed picture of the pathogenesis of acute MEV-related disease. Moreover, the data are correlated with information obtained previously from the study of the other mink parvovirus, Aleutian mink disease parvovirus (ADV), which causes both acute and chronic disease in mink (6).

The serological response to MEV infection and the levels of virus shedding in feces have been investigated before (7, 32, 36). However, the viral distribution during the infection has been examined only by Parrish et al. (25), who measured PFUs on PID 5. Therefore, because of the limited number of reports on MEV pathogenesis, we will base our comparisons on observations made on the closely related CPV infection in dogs.

The histopathological changes found in infected mink in this study were similar to those described by others (7, 15, 21, 33) and will be discussed only in relation to the in situ hybridization data.

The specific antibody titers in serum resemble those of our earlier reports (36). Briefly, significant increases in serum titers can be detected from PID 6 or 8. In addition, bile had titers at least as high as those of sera. This indicated that both the systemic and the local intestinal antibody responses to MEV are fast and may influence the rapid decline in MEV replication and shedding observed.

Fecal shedding of MEV was detectable from PID 4 by using ELISA and was detectable in a single mink from PID 2 by using nucleic acid hybridization with a ^{32}P-labeled RNA probe. On PID 8, both mink were positive for MEV nucleic acid but negative by ELISA, as reported earlier (25, 36). Together with the antibody data, this suggests to us that the hybridization technique is more sensitive than ELISA and that the hybridization technique can detect virus in late

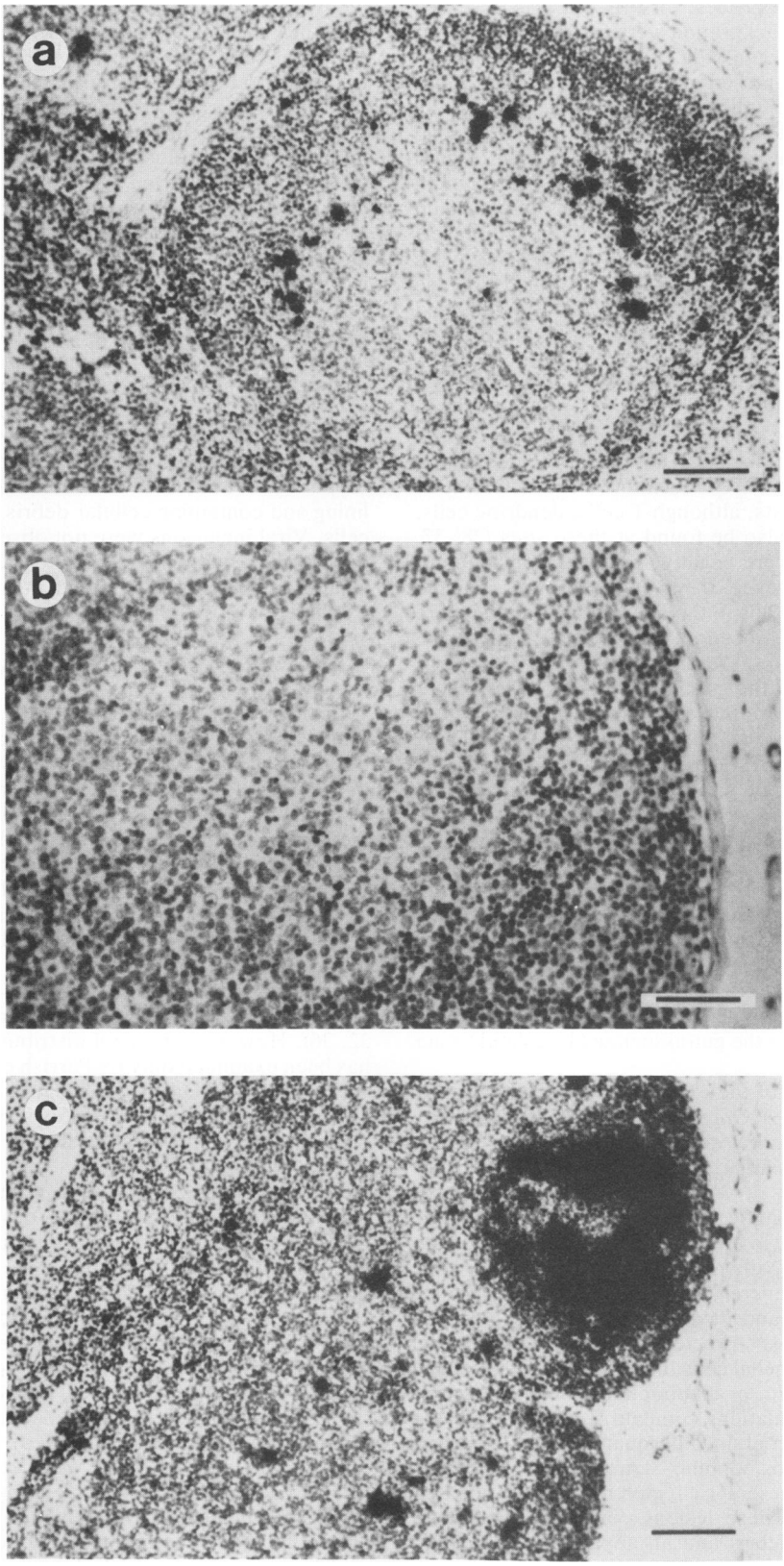

FIG. 6. In situ hybridization analysis of sections of mesenteric lymph node from mink infected with MEV. (a) In situ hybridization analysis of sections of mesenteric lymph node from a mink infected with MEV for 4 days. The section was hybridized with the minus-sense probe. Heavy grain production is seen over cells in the periphery of the central zone of a lymph node follicle. Bar, 80 μm. (b) In situ hybridization analysis of sections of mesenteric lymph node from mink infected with MEV for 8 days. The section was hybridized with the minus-sense probe. Only background levels of grains can be observed over a follicle. Bar, 50 μm. (c) In situ hybridization analysis of sections of mesenteric lymph node from mink infected with MEV for 8 days. The section was hybridized with the plus-sense probe. Heavy grain production is observed over scattered single cells in the cortex and over a follicle. Bar, 80 μm.

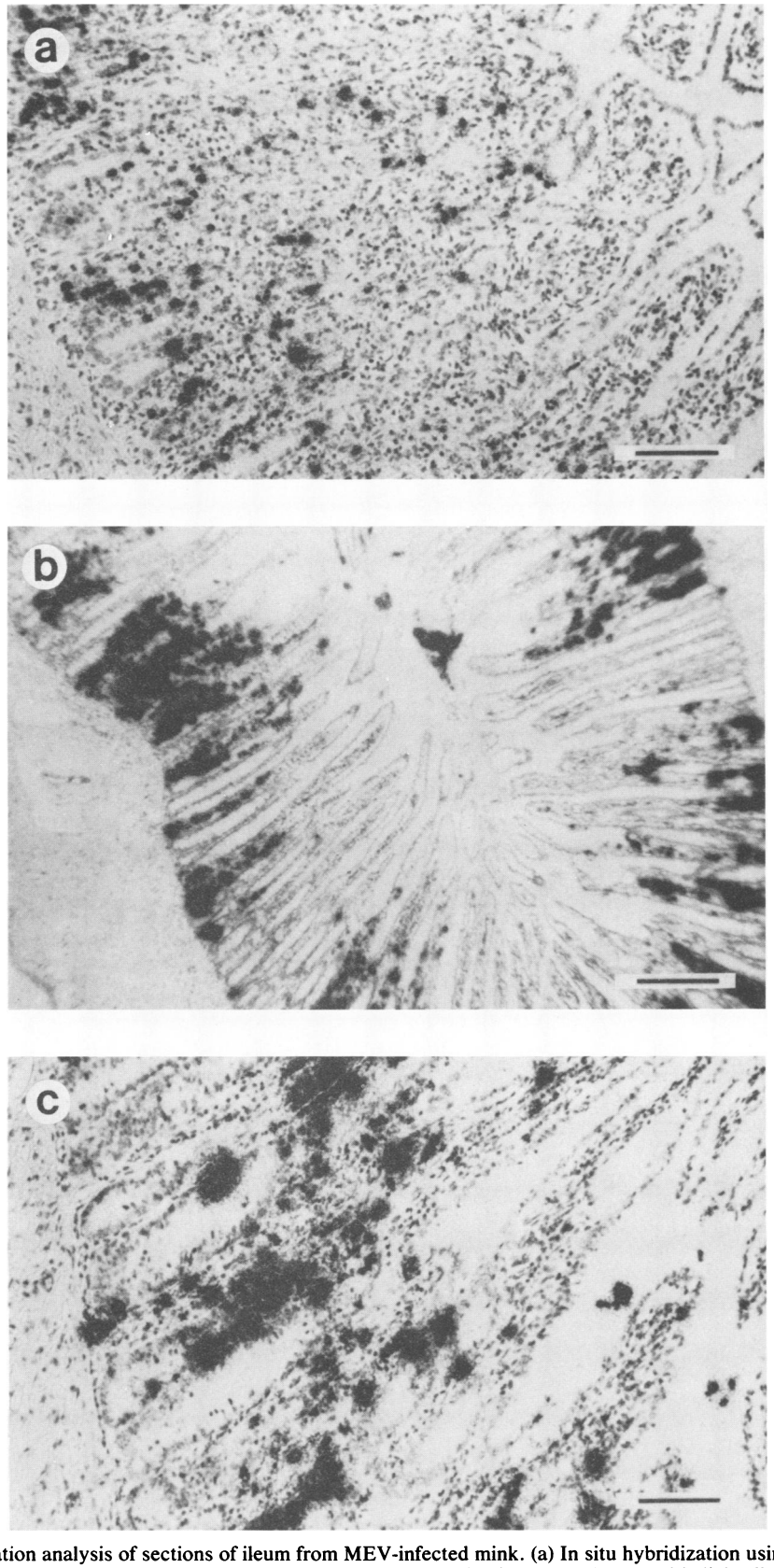

FIG. 7. In situ hybridization analysis of sections of ileum from MEV-infected mink. (a) In situ hybridization using the minus-sense probe on ileum section from a mink infected with MEV for 4 days. Heavy grain production is observed over epithelial cells in the crypts and on villi. Bar, 80 μm. (b and c) In situ hybridization using the plus-sense probe on ileum section from a mink infected with MEV for 6 days. Heavy grain production is seen in the lumen of the intestine and over focal areas of the crypts and villi. Bars, 230 μm (b) and 80 μm (c).

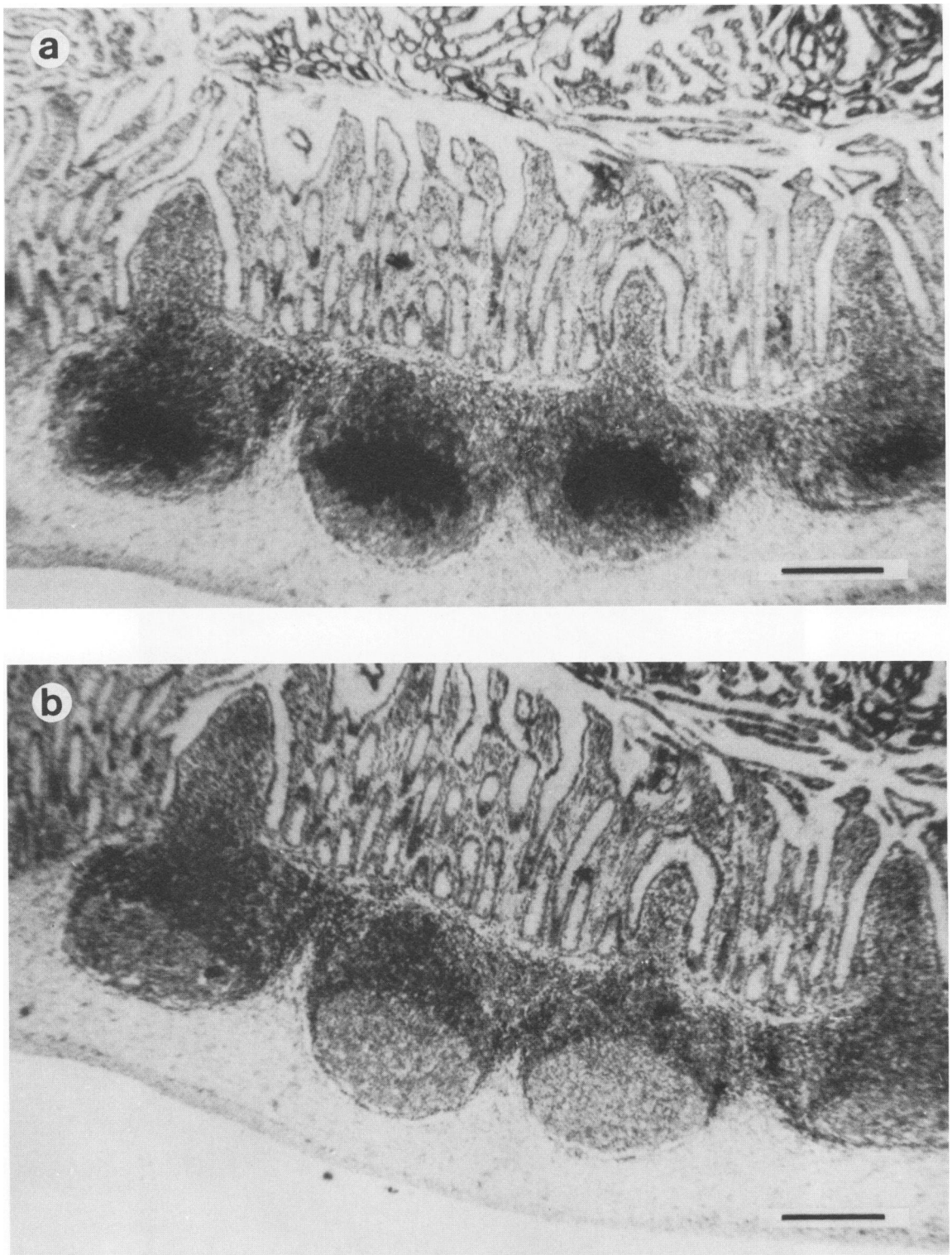

FIG. 8. In situ hybridization analysis of ileum sections from a mink infected with MEV for 8 days. Sections were hybridized with the plus-sense probe (a) or the minus-sense probe (b). Grain production is evident with the plus-sense probe and is located over the gut-associated lymphoid tissue. Bars, 230 μm.

TABLE 1. In situ hybridization analysis of ileum sections from mink[a]

Time (days) p.i.	% of cells scored positive		Genomes per[b]:			
			Positive cell		Total cell	
	RF probe	Virion probe	RF probe	Virion probe	RF probe	Virion probe
0	0	0	<300	<300	ND	ND
2	0.1	0.1	50,000	50,000	50	50
4	5	5	250,000	70,000	12,500	3,500
6	2	10	250,000	100,000	5,000	10,000
8	0.1	2	50,000	100,000	50	2,000

[a] Mink were inoculated with a MEV inoculum, and two mink were killed at each of the indicated times. Zero days indicates uninfected controls. Sections of ileum were processed for in situ hybridization analysis as described in Materials and Methods. The number of positive cells and number of grains over each positive cell were recorded for an area containing 20 positive cells or a total of at least 10,000 cells.

[b] The number of genomes per positive cell and total cell was estimated by comparison with an included standard of MEV-infected CRFK cells, as described previously (4–6). ND, Not determined.

infection where ELISA fails, probably because of coating of the virions with antibody. In other studies, ELISA was compared with DNA hybridization for detection of CPV in fecal samples from dogs (35). The studies showed a correlation of 73% and concluded, similarly, that the hybridization technique was more sensitive than ELISA.

The mink in this study were inoculated by the oronasal route. By using in situ hybridization, actively replicating MEV was detected with both probes in the mesenteric lymph node and ileum at PID 2, before histological examination revealed any lesions. Typical histological lesions of early MEV infection, the peak of viral replication, and the onset of virus shedding in feces coincided and were found in the animals killed on PID 4. Viral replication detected by in situ hybridization decreased rapidly and was at low levels when viral inclusion bodies were abundant (PIDs 6 and 8). This may indicate that the inclusion bodies are residual lesions after virus replication and consist of virions, viral proteins or nucleic acids, or cellular components.

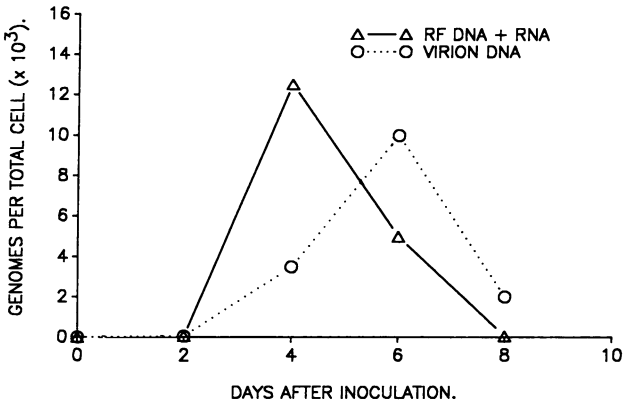

FIG. 9. Estimation of genomes per total cell in ileum sections by in situ hybridization. In situ hybridization was performed on PLPG-fixed paraffin-embedded tissue as described in Materials and Methods. Cells containing virion DNA were detected by using the plus-sense probe, and RF DNA and mRNA were detected by using the minus-sense probe on slides not treated with RNase. The number of genomes per total cell was calculated by multiplying the content of genomes per positive single cell by the percentage of positive cells, as described previously (4–6).

The viral sequences on PID 6 were detected mainly in intestinal sections and lymphoid tissue by the plus-sense probe, as a nonreplicating virus. At this time, low levels of sequestered MEV virion DNA were detectable in the liver. In the other sections examined, no viral sequences could be detected. At PID 8, the level of viral replication was very low. However, virion DNA could be detected in up to 2% of the cells. This indicated that the acute phase of viral replication was over and that the animals were recovering from the infection, even though histological examination still revealed tissue lesions. In dogs, CPV is present in all lymphoid, parenchymatous, and intestinal tissues by day 4. On day 8, infectious virus could no longer be isolated (12). These data are in accordance with ours. Earlier results on MEV infection on the basis of pathoanatomical features (15) suggested a degenerative phase on PIDs 7 through 11 followed by a regenerative phase on PIDs 12 through 21 after MEV infection in mink. The results of the present study suggested that the acute period of active MEV replication is even shorter than that originally expected, i.e., only PIDs 2 through 6. Thus, lesions seen after this period probably represent regenerative changes and repair and perhaps desquamation of cells damaged at an earlier point of infection.

Cell-free viremia (corresponding to approximately 1 ng of MEV virion DNA per ml of serum) was detected in one of two animals on PIDs 2 and 4. One animal that died on PID 6 (6C) had high antibody titers against MEV and a high level of viremia, i.e., about 10 ng of virion DNA per ml of serum. All other serum samples collected on PIDs 6 and 8 were negative for viral sequences. These data suggest that the mink did die from the virus challenge and support previous reports on CPV infection in dogs, in which the magnitude of viremia had a strong positive correlation with the severity of clinical disease (20). The viremia in our study was not apparent by hemagglutination assay (HA) (data not shown). These findings may indicate that the HA test is not sensitive enough to detect these levels of virus or that the viremic phase is accompanied by the production of antibodies that inhibit the HA. Data from dogs experimentally infected with CPV suggest a transient viremic phase on PIDs 2 through 4. The serum samples were tested by isolation of virus in cell culture (20), and it is possible that antibodies in serum samples, detected from day 3, neutralized the cell-free virus in later samples.

The viremic state in MEV as in CPV infection is an early transient phase unless the animal succumbs to the disease. The fact that the viremic phase on PIDs 2 through 4 is observed before the peak of viral replication detected in the tissues may indicate that the oronasal infection is spreading from a primary site of infection (most probably lymphoid tissue) via blood or lymph to the sites of infection in lymph nodes and intestinal epithelial cells. This idea is supported by similar data on CPV infection in dogs (26).

In our previous work using in situ hybridization analysis of tissue sections from mink infected with the other mink parvovirus, ADV (4–6), calculations of the amount of ADV-specific virion DNA, RFs of DNA, and mRNA present were made. The amount of ADV RFs of DNA and mRNA in mesenteric lymph node cells at the peak of infection of adult mink (PID 10) reached only 10,000 genomes per infected cell, while alveolar type II cells from mink kits neonatally infected with ADV contained up to 400,000 genomes per infected cell. The results presented here suggested that for MEV infection, the number of genomes per infected intestinal epithelial cell or lymph node cell is approximately 250,000, i.e., a level resembling the amount present in the

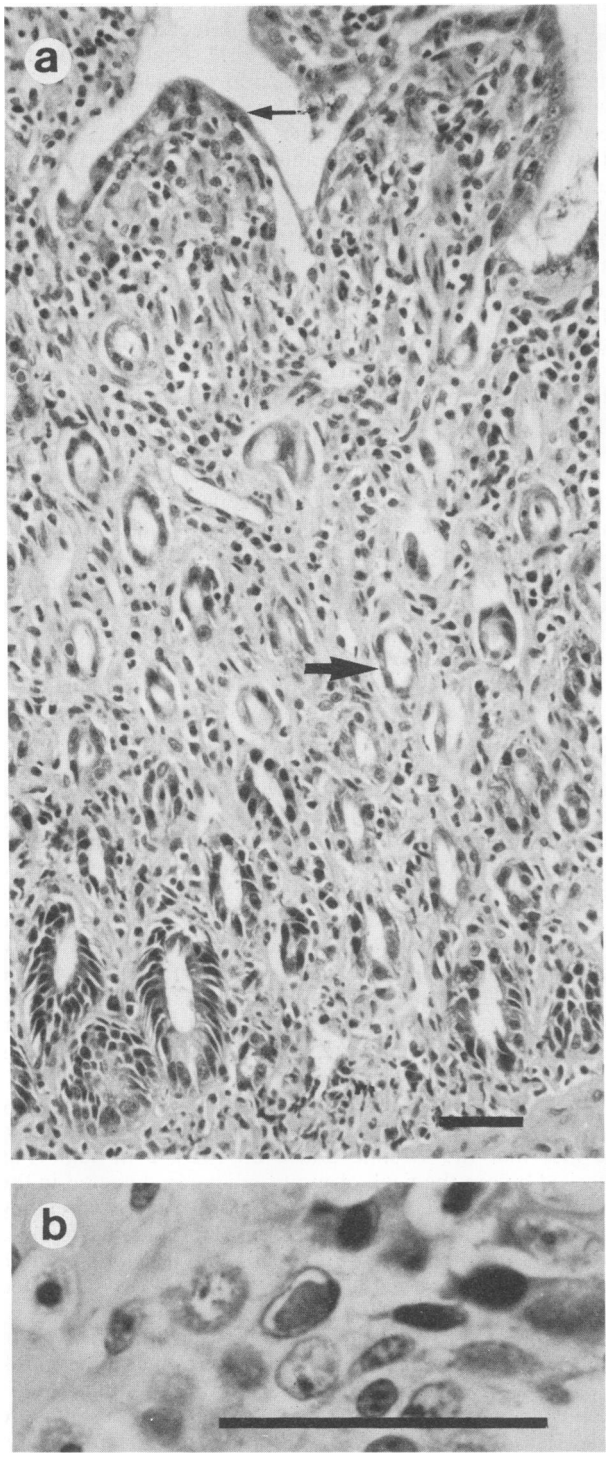

FIG. 10. Mucosal lesions in the small intestine of MEV-infected mink on PID 6. (a) Villi are short, plump, and irregular and covered by fewer than normal and flattened epithelial cells (thin arrow). Most crypts are atrophic and lined by attenuated epithelium (thick arrow) because of loss of crypt epithelial cells. (b) Intranuclear viral inclusion in crypt epithelial cell. Bars, 50 μm.

permissive ADV lung system. This level of viral replication in individual infected cells probably has an impact on acute cellular lesions and development of clinical disease. Adult mink infected with ADV have no acute clinical or histopathological signs of disease, whereas mink kits infected neonatally develop an acute, fatal, interstitial pneumonia within 10 to 15 days after infection. Three- to five-month-old mink experimentally infected with MEV have 10 to 20% mortality on PIDs 5 through 10 (36) and do have histopathological evidence of acute cellular lesions.

The levels of MEV RFs of DNA and mRNA reached peak levels at PID 4 in this experiment, 2 days before the maximal amount of virion DNA was detected. In cell culture, MEV infection could be detected already at 10 h p.i. and viral replication reached maximal levels at 24 h p.i. In contrast, ADV replication and virus sequestration reach maximal levels at 10 to 14 days after infection of both neonatal and adult mink (4–6). In cell culture, ADV replication can be detected at 24 h p.i. but does not reach maximal levels before 96 h p.i. (5) even when cultured under the same conditions as MEV (S. Alexandersen and M. E. Bloom, unpublished observations). These data suggest that ADV replication per se is slower than MEV replication and that this decrease in speed of replication has an impact on the pathogenesis of disease observed. We have previously hypothesized that the decreased level of ADV replication seen in adult mink is due to antiviral antibodies (4, 6). Therefore, it is tempting to speculate that acute cellular lesions and clinical disease caused by mink parvoviruses is linked to either a weak or slow antibody response, i.e., ADV infection of neonatal mink kits, or a fast-replicating virus capable of replicating to high levels before the onset of an antibody response, i.e., MEV infection. This would also explain why immunized animals are insusceptible to MEV infection and why young mink, with a poorly developed immune response, have a higher mortality rate than older mink when infected with MEV. In contrast, ADV infection of adult mink is slow, allowing sufficient time for a high-level antibody response, resulting in decreased levels of viral replication and thereby preventing the development of acute lesions. However, the mechanisms for the development of a continued low-level persistent infection in adult ADV-infected mink are still obscure.

In conclusion, our results stress the remarkable differences between the two mink parvovirus infections. In the classical adult ADV infection, the incubation period is much longer and the maximal number of genomes per infected cell is severely depressed and is present at PID 10 when no clinical signs of disease are evident. Furthermore, the actual tissue damage caused by this disease is due to immune disorders and appears several months or years after infection (4, 27). In contrast, in the ADV-induced interstitial pneumonia affecting mink kits and in MEV infection of adult mink, the high-level peak of viral replication most likely induces cellular lesions leading to acute clinical disease. Further studies on the molecular pathogenesis of mink parvovirus-induced disease are in progress.

ACKNOWLEDGMENTS

The assistance of Lene Arndrup is greatly appreciated.

This research was supported by the Danish Fur Breeders Association Research Foundation, the Danish Animal Biotechnology Research Center, the Danish Council for Veterinary and Agricultural Research, and the U.S. Department of Health and Human Services, National Institutes of Health (NIH).

LITERATURE CITED

1. **Aasted, B., and A. Cohn.** 1982. Inhibition of precipitation in counter current electrophoresis. A sensitive method for detection of mink antibodies to Aleutian disease virus. Acta Pathol. Microbiol. Immunol. Scand. Sect. C **90**:15–19.
2. **Alexandersen, S., and M. E. Bloom.** 1987. Studies on the sequential development of acute interstitial pneumonia caused by Aleutian disease virus in mink kits. J. Virol. **61**:81–86.
3. **Alexandersen, S., M. E. Bloom, and S. Perryman.** 1988. Detailed transcription map of Aleutian mink disease parvovirus. J. Virol. **62**:3684–3694.
4. **Alexandersen, S., M. E. Bloom, and J. Wolfinbarger.** 1988. Evidence of restricted viral replication in adult mink infected with Aleutian disease of mink parvovirus. J. Virol. **62**:1495–1507.
5. **Alexandersen, S., M. E. Bloom, J. Wolfinbarger, and R. E. Race.** 1987. In situ molecular hybridization for detection of Aleutian mink disease parvovirus DNA by using strand-specific probes: identification of target cells for viral replication in cell cultures and in mink kits with virus-induced interstitial pneumonia. J. Virol. **61**:2407–2419.
6. **Alexandersen, S., S. Larsen, A. Cohn, Å. Uttenthal, R. E. Race, B. Aasted, M. Hansen, and M. E. Bloom.** 1989. Passive transfer of antiviral antibodies restricts replication of Aleutian mink disease parvovirus in vivo. J. Virol. **63**:9–17.
7. **Barker, I., C. Povey, and D. Voight.** 1983. Response of mink, skunk, red fox and raccoon to inoculation with mink virus enteritis, feline panleucopenia and canine parvovirus and prevalence of antibody to canine parvovirus in wild carnivores in Ontario. Can. J. Comp. Med. **47**:188–197.
8. **Blixenkrone-Møller, M., E. Lund, G. Mikkelsen, and Å. Uttenthal.** 1987. Blood collection in mink. Scand. J. Lab. Anim. Sci. **14**:99.
9. **Bloom, M. E., S. Alexandersen, S. Mori, and J. B. Wolfinbarger.** 1989. Analysis of parvovirus infections using strand-specific hybridization probes. Virus Res. **14**:1–26.
10. **Bloom, M. E., R. E. Race, B. Aasted, and J. B. Wolfinbarger.** 1985. Analysis of Aleutian disease virus infection in vitro and in vivo: demonstration of Aleutian disease virus DNA in tissues of infected mink. J. Virol. **55**:696–703.
11. **Bloom, M. E., R. E. Race, and J. B. Wolfinbarger.** 1987. Analysis of Aleutian disease of mink parvovirus infection using strand specific hybridization probes. Intervirology **27**:102–111.
12. **Carman, P. S., and R. C. Povey.** 1985. Pathogenesis of canine parvovirus-2 in dogs: hematology, serology and virus recovery. Res. Vet. Sci. **38**:134–140.
13. **Cho, H. J., and D. G. Ingram.** 1972. Antigen and antibody in Aleutian disease in mink. I. precipitation reaction by agar-gel electrophoresis. J. Immunol. **108**:555–557.
14. **Johnson, R. H., G. Siegl, and M. Gautschi.** 1974. Characteristics of feline panleukopenia virus strains enabling definitive classification as parvoviruses. Arch. Gesamte Virusforsch. **46**:315–324.
15. **Krunajevic, T.** 1970. Experimental virus enteritis in mink: a pathologic-anatomical and electron microscopical study. Acta Vet. Scand. Suppl. **30**:1–88.
16. **MacPherson, L.** 1956. Feline panleucopenia virus—its transmission to mink under natural and experimental conditions. Can. J. Comp. Med. **20**:197–202.
17. **McAdaragh, J., S. Eustis, D. Nelson, I. Stotz, and K. Kenefick.** 1982. Experimental infection of conventional dogs with canine parvovirus. Am. J. Vet. Res. **43**:693–696.
18. **McMaster, G., J. Tratschin, and G. Siegl.** 1981. Comparison of canine parvovirus with mink enteritis virus by restriction site mapping. J. Virol. **38**:368–371.
19. **Meunier, P., B. Cooper, M. Appel, M. Lanieu, and D. Slauson.** 1985. Pathogenesis of canine parvovirus enteritis: sequential virus distribution and passive immunization studies. Vet. Pathol. **22**:617–624.
20. **Meunier, P., B. Cooper, M. Appel, and D. Slauson.** 1985. Pathogenesis of canine parvovirus enteritis: the importance of viremia. Vet. Pathol. **22**:60–71.
21. **Myers, W., and T. Fritz.** 1956. Histopathologic changes in virus enteritis of mink. Can. J. Comp. Med. **23**:246–249.
22. **Parrish, C. R., C. F. Aquadro, and L. E. Carmichael.** 1988. Canine host range and a specific epitope map along with variant sequences in the capsid protein gene of canine parvovirus and related feline, mink, and raccoon parvoviruses. Virology **166**: 293–307.
23. **Parrish, C. R., and L. E. Carmichael.** 1986. Characterization and recombination mapping of an antigenic and host range mutation of canine parvovirus. Virology **148**:121–132.
24. **Parrish, C. R., J. R. Gorham, T. Schwartz, and L. E. Carmichael.** 1984. Characterization of antigenic variation among mink enteritis virus isolates. Am. J. Vet. Res. **45**:2591–2599.
25. **Parrish, C. R., C. W. Leathers, R. Pearson, and J. R. Gorham.** 1987. Comparisons of feline panleukopenia virus, canine parvovirus, raccoon parvovirus, and mink enteritis virus and their pathogenicity for mink and ferrets. Am. J. Vet. Res. **48**: 1429–1435.
26. **Pollock, R.** 1982. Experimental canine parvovirus infection in dogs. Cornell Vet. **72**:103–119.
27. **Porter, D. D., A. E. Larsen, and H. G. Porter.** 1969. The pathogenesis of Aleutian disease of mink. I. In vivo viral replication and the host antibody response to viral antigen. J. Exp. Med. **130**:575–589.
28. **Raviola, E.** 1986. The immune system, p. 406–478. *In* W. Bloom and D. W. Fawcett (ed.), A textbook of histology. The W. B. Saunders Co., Philadelphia.
29. **Reed, A. P., E. V. Jones, and T. J. Miller.** 1988. Nucleotide sequence and genome organization of canine parvovirus. J. Virol. **62**:266–276.
30. **Reynolds, H.** 1970. Pathological changes in virus enteritis of mink. Can. J. Comp. Med. **34**:155–163.
31. **Rhode, S. L., III.** 1985. Nucleotide sequence of the coat protein gene of canine parvovirus. J. Virol. **54**:630–633.
32. **Rivera, E., and K.-A. Karlsson.** 1987. A solid-phase fluorescent immunoassay for detecting canine or mink enteritis parvoviruses in faecal samples. Vet. Microbiol. **15**:1–9.
33. **Schofield, F.** 1949. Virus enteritis in mink. N. Am. Vet. **30**: 651–654.
34. **Siegl, G., R. C. Bates, K. I. Berns, B. C. Carter, D. C. Kelly, E. Kurstak, and P. Tattersall.** 1985. Characteristics and taxonomy of parvoviridae. Intervirology **23**:61–73.
35. **Teramoto, Y. A., M. M. Mildbrand, J. Carlson, J. K. Collins, and S. Winston.** 1984. Comparison of enzyme-linked immunosorbent assay, DNA hybridization, hemagglutination, and electron microscopy for detection of canine parvovirus infections. J. Clin. Microbiol. **20**:373–378.
36. **Uttenthal, Å.** 1988. Apparent lack of effect of vaccination against mink enteritis virus (MEV). A challenge study. Arch. Virol. **99**:153–161.
37. **Witmer, M. D., and R. M. Steinman.** 1984. The anatomy of peripheral lymphoid organs with emphasis on accessory cells: light microscopic immunocytochemical studies of mouse spleen, lymph node, and Peyers' patch. Am. J. Anat. **170**: 465–481.
38. **Yoffey, J. M., and I. A. Olsen.** 1967. The formation of germinal centers in the medulla of lymph nodes, p. 41–48. *In* H. Cottier, N. Odartchenko, R. Schindler, and C. C. Congdon (ed.), Germinal centers in immune response. Springer-Verlag, New York.